

6-Carboxycellulose Acetate Butyrate: Effectiveness as an Amorphous Solid Dispersion Polymer

Published as part of Molecular Pharmaceutics *virtual special issue* "Pharmaceutical Sciences and Drug Delivery Research from Early Career Scientists".

Joyann A. Marks,* Brittany L. B. Nichols, Laura I. Mosquera-Giraldo, Sara T. Yazdi, Lynne S. Taylor, and Kevin J. Edgar



Cite This: *Mol. Pharmaceutics* 2024, 21, 4589–4602



Read Online

ACCESS |

Metrics & More

Article Recommendations

Supporting Information

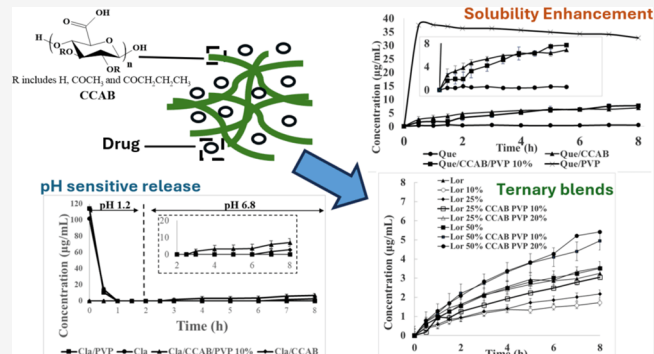
ABSTRACT: Amorphous solid dispersion (ASD) in a polymer matrix is a powerful method for enhancing the solubility and bioavailability of otherwise crystalline, poorly water-soluble drugs. 6-Carboxycellulose acetate butyrate (CCAB) is a relatively new commercial cellulose derivative that was introduced for use in waterborne coating applications. As CCAB is an amphiphilic, carboxyl-containing, high glass transition temperature (T_g) polymer, characteristics essential to excellent ASD polymer performance, we chose to explore its ASD potential. Structurally diverse drugs quercetin, ibuprofen, ritonavir, loratadine, and clarithromycin were dispersed in CCAB matrices. We evaluated the ability of CCAB to create ASDs with these drugs and its ability to provide solubility enhancement and effective drug release.

CCAB/drug dispersions prepared by spray drying were amorphous up to 25 wt % drug, with loratadine remaining amorphous up to 50% drug. CCAB formulations with 10% drug proved effective at providing *in vitro* solubility enhancement for the crystalline flavonoid drug quercetin as well as ritonavir, but not for the more soluble APIs ibuprofen and clarithromycin and the more hydrophobic loratadine. CCAB did provide slow and controlled release of ibuprofen, offering a simple and promising Long-duration ibuprofen formulation. Formulation with clarithromycin showed the ability of the polymer to protect against degradation of the drug at stomach pH. Furthermore, CCAB ASDs with both loratadine and ibuprofen could be improved by the addition of the water-soluble polymer poly(vinylpyrrolidone) (PVP), with which CCAB shows good miscibility. CCAB provided solubility enhancement in some cases, and the slower drug release exhibited by CCAB, especially in the stomach, could be especially beneficial, for example, in formulations containing known stomach irritants like ibuprofen.

KEYWORDS: *ternary blends, carboxy cellulose ester, solubility enhancement, amorphous solid dispersion, structural diversity, loratadine*

1. INTRODUCTION

Polymer matrix materials are vital components of modern drug delivery systems, being used to modify release rates, provide pH-responsiveness, counteract bad tasting active pharmaceutical ingredients (APIs), and provide other benefits.^{1–3} Cellulose derivatives have been especially useful in drug delivery due to beneficial features including generally low toxicity, compatibility with various drug actives, and an essentially complete lack of oral bioavailability. Some derivatives have good organic solubility and some are thermoplastic, enabling simple processing into micro- and nanoparticulate materials.⁴ Cellulose esters in particular have been heavily used in commercial drug formulations, given their ability to be processed by many methods (e.g., film casting,^{4–6} spray drying,^{7–10} extrusion^{11–13}). Certain commercial cellulose ether esters that were designed for other purposes have been



found to be effective ASD polymers (for example hydroxypropyl methyl cellulose acetate succinate (HPMCAS)^{4,7,9,14–20} and carboxymethyl cellulose acetate butyrate (CMCAB)^{5,7,9,15,21–23}), while other cellulose esters have been specifically designed to be effective ASD polymers (e.g., cellulose acetate adipate propionate (CAAdP),^{7,9,14,24} cellulose acetate suberate (CASub),^{14,25,26} and 5-carboxypentyl hydroxypropyl cellulose).^{27–29}

Received: May 3, 2024

Revised: July 26, 2024

Accepted: July 29, 2024

Published: August 1, 2024



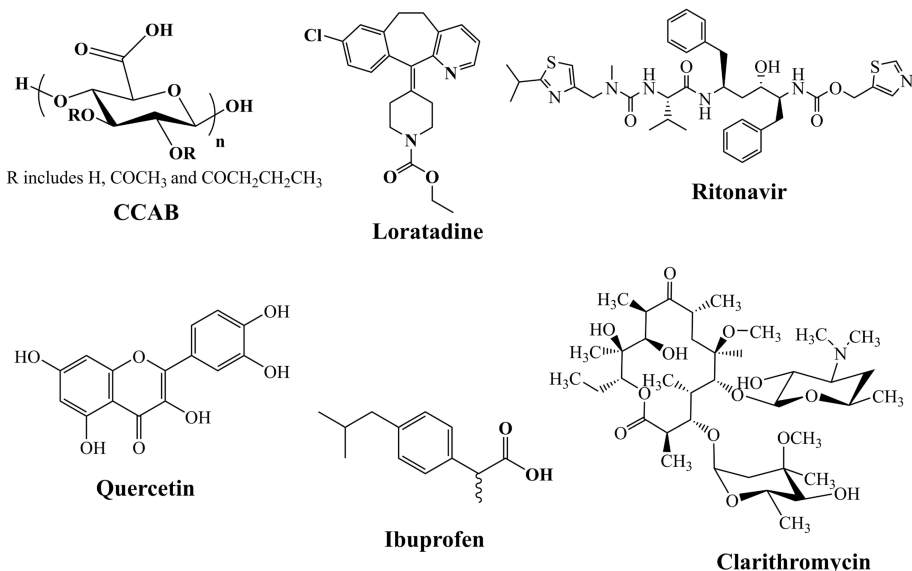


Figure 1. Chemical structures of polymers and pharmaceuticals used.

The Taylor and Edgar laboratories have collaborated to design novel cellulose-based polymers for ASD to address performance issues with currently utilized ASD polymers (e.g., poly(vinylpyrrolidone) (PVP), poly(acrylic acid), HPMC, HPMCAS) that were not originally designed as ASD polymers. ASDs comprise molecular dispersions of drugs in a polymer that maintain the drug in a high energy, amorphous state by entrapping the drug in an amorphous glass and by reducing the energy of the amorphous drug through constructive polymer-drug interactions. ASDs generate supersaturated drug solutions upon drug release, thereby potentially defeating both solubility and permeation barriers to bioavailability (permeation rate being enhanced by the increased drug chemical potential difference across the membrane, caused by supersaturation).^{30–32} The ASD polymer component is required to play several roles; stabilizing the drug in the solid and solution phases through hydrogen bonding and other interactions, retaining the glassy solid state, and releasing the drug at an adequate rate.³³ We can define polymer structural elements important to success in ASD, including possessing moieties capable of hydrogen bonding (H-bonding) with the drug, a balance of hydrophobicity and hydrophilicity (amphiphilicity), which impacts miscibility with the drug and proper balance of drug and polymer dissolution rates,^{24,26,34} and high glass transition temperature (T_g). Many cellulose esters have high T_g values, and this helps to retard recrystallization by maintaining the glassy state, thus limiting drug mobility even in the presence of water plasticization at high humidity and/or due to drug that may also be a plasticizer. We seek to innovate polymers tailored for ASD in order to improve performance of existing drugs and bring new drugs to market that would otherwise fail due to poor solubility and bioavailability. At the same time, by understanding polymer features needed for ASD performance, we may recognize some polymers created for other purposes but potentially useful for ASD. Such multiuse polymers are particularly attractive since they are more likely to thrive in the market and thus remain available for use in ASDs.

One such commercial polymer of interest is modified celluronic acid, 6-carboxycellulose acetate butyrate, or CCAB (alternatively named celluronic acid acetate butyrate). CCAB was introduced by the Eastman Chemical Company³⁵ for

water-dispersion applications, but there are no detailed reports of its utility in drug delivery, nor specifically in ASD. The short to medium chain length ester groups (degree of substitution (DS) butyryl 1.62, acetyl 0.06) of CCAB provide hydrophobicity, while its oxidation at C-6 to the uronic acid (carboxyl DS 0.28) provides pH-responsiveness, and polarity at neutral pH and higher. Carboxyl content is important, not only for favorable H-bonding interactions with drug actives but also to drive drug release in the intestine, triggered by carboxyl ionization and resulting polymer swelling and/or dissolution. We therefore hypothesize that the amphiphilic cellulose derivative CCAB could be a useful ASD polymer, providing enhanced solubility to a variety of poorly soluble drug actives and thereby enhancing bioavailability. We further hypothesize that the amphiphilic nature of CCAB will afford strong interactions between polymer and hydrophobic drugs, thereby providing a simple system for extended release formulations of such drugs (and potentially simultaneously enhancing solubility).

We have chosen to study the ASD properties of CCAB using several structurally diverse model drugs, each of which has poor aqueous solubility under at least some conditions; ibuprofen (Ibu, anti-inflammatory),^{36–38} loratadine (Lor, antihistamine),³⁹ quercetin (Que, antioxidant flavonoid),^{7,40} ritonavir (Rit, antiretroviral),⁴¹ and clarithromycin (Cla, antibiotic).⁹ Besides their structural diversity, they are also diverse in terms of their therapeutic use. We describe herein formation of dispersions with these model drugs, analysis of the degree of crystallinity of each drug at various drug levels in the dispersion, and solubility and release characteristics of each drug from these CCAB dispersions, allowing us to make conclusions about the utility of CCAB as an ASD polymer.

2. EXPERIMENTAL SECTION

2.1. Materials. Methanol, ethanol, dichloromethane, acetone, acetonitrile, and tetrahydrofuran (THF) were purchased from Fisher Scientific, Pittsburgh, PA and used as received. CCAB (MW 252,300, determined using size exclusion chromatography (SEC) as described below), DS (butyrate) 1.62, DS (acetate) 0.03 (both by ^1H NMR, see below), DS (CO_2H) 0.28 (determined by manufacturer) was

from Eastman Chemical Company (Kingsport, Tennessee). Molecular weight determination was by SEC in DMAc containing 0.1% LiCl using a Waters 1515 isocratic HPLC pump, a Viscotek 270 dual detector, and a Waters 2414 refractive index detector. DS was measured by ¹H NMR spectroscopy (Bruker AVANCE 500 MHz) in *d*₆-DMSO (NMR data and DS calculations can be found in Supporting Information, Figure S1). PVP (K29/32) was obtained from Sigma-Aldrich. Ibu and Lor were purchased from LKT Laboratories, St. Paul, Minnesota, USA, and Oakwood Chemicals, Estill, South Carolina, USA, respectively. Que (hydrate, ≥ 95%) was purchased from Aldrich Chemicals, Saint Louis, Missouri, USA, Cla (≥98%) was from TCI Chemicals, Kita-Ku, Tokyo, Japan, and Rit was from Attix Pharmaceuticals, Toronto, Ontario, Canada.

2.2. Preparation of Solid Dispersions. Samples were prepared on a Buchi Mini B-290 spray dryer under nitrogen. Each polymer/drug pair (1–2 g) was mixed in the ratios 9:1, 4:1, and 1:1 (w:w, polymer:drug) and subsequently dissolved in 50–100 mL of solvent (methanol for Ibu, Rit and Cla, acetonitrile for Lor, ethanol for Que). We employed spray dryer settings of the pump at 45%, aspirator at 100%, and inlet temperatures of 90 °C to produce polymer/drug blends as powders. The temperature was set at least 10 °C above the solvent boiling point. Physically mixed CCAB/drug 10% formulations were also prepared for comparison of relative crystallinity and thermal properties. These physical mixtures containing weighed portions (9:1 w:w polymer: drug) of CCAB and drug were ground in a mortar and pestle, and the resulting powder was used as physical mixture negative controls.

2.3. Differential Scanning Calorimetry (DSC). Heating curves of 4–10 mg of spray-dried powder samples in TA Instruments Tzero aluminum pans were obtained on a TA Instruments Q2000 DSC or TA discovery DSC (New Castle, DE). Samples were first equilibrated at −75 °C for 5 min followed by heating at 20 °C/min to 160 or 200 °C. Samples were quench-cooled at 100 °C/min to −75 °C and then reheated at the same rate. Second heating scan thermograms were evaluated to obtain *T*_g values. The TA Universal Analysis 2000 was used to evaluate the glass transition temperatures after establishing the limits before and after the step in the heat flow trace (limits were ~50 °C before and after the onset and endset points). Where necessary, samples were subjected to temperature-modulated DSC (MDSC) with a heating rate of 4 °C/min from −50 to 150 or 180 °C and a modulation amplitude of ±0.5 °C for 40 s. For these samples, reversing heat flow thermograms were evaluated.

2.4. Proton Nuclear Magnetic Resonance Spectroscopy (¹H NMR). ¹H NMR spectra were obtained at 22 °C on Bruker AVANCE 500 MHz spectrometers in DMSO-*d*₆ using 16 scans, with 2 drops of TFA added to shift the HOD peak of DMSO- *d*₆ downfield from the spectral region of interest. Chemical shifts are reported relative to the solvent peaks.

2.5. Fourier Transform Infrared Spectroscopy (FTIR). Infrared spectra were obtained on spray-dried powder samples in absorbance mode using a Bio-Rad FTS 6000 spectrophotometer equipped with a globar infrared source, KBr beam splitter, and DTGS (d-triglycine sulfate) detector. Spectra of the powdered samples were obtained using a Golden Gate MII attenuated total reflectance (ATR) sampling accessory with a diamond top plate (Specac Inc., Woodstock, GA) to which a thin layer of powdered sample was added. The scan range was

set from 4000 to 500 cm^{−1} with a 4 cm^{−1} resolution, and 128 scans were coadded. The absorbance intensity of the spectral region of interest was between 0.6 and 1.2.

2.6. X-ray Diffraction (XRD). Crystallinity was analyzed using powder X-ray diffraction (XRD) for both spray-dried and physically mixed samples. XRD patterns were obtained using a Shimadzu XRD 6000 diffractometer (Shimadzu Scientific Instruments, Columbia, Maryland). The geometry of the X-ray diffractometer was the Bragg–Brentano parafocusing. The instrument was calibrated using a silicon standard that has a characteristic peak at 28.44° 2θ. The X-ray tube consisted of a target material made of copper (Cu), which emits Kα radiation with a power rating of 2200 W and accelerating potential of 60 kV. Experiments were performed using a 40 kV accelerating potential and current of 30 mA. Divergence and scattering slits were set at 1.0 mm and the receiving slit at 10 iris. The experiments were conducted with a scan range from 10 to 50° 2θ. The scanning speed was 5°/min. Comparisons of spray-dried and physically mixed dispersions containing 10% drug are provided in Figure S2.

2.7. Size Exclusion Chromatography (SEC). Molecular weights were determined by SEC in DMAc containing 0.1% LiCl using a Waters 1515 isocratic HPLC pump, a Viscotek 270 dual detector, and a Waters 2414 refractive index detector. The mobile phase flow rate was 0.5 mL/min. Universal calibration curves were prepared by using polystyrene standards.

2.8. Drug Quantification by Ultraviolet–Visible Spectroscopy (UV–vis) and High-Performance Liquid Chromatography with Diode–Array Detection (HPLC-DAD). All UV–vis spectra were recorded on a Thermo Scientific Evolution 300 UV–visible Spectrometer. Standard curves were generated for each drug in an appropriate solvent (methanol for Ibu and Rit, ethanol for Que, and acetonitrile for Lor) and utilized to calculate the concentration of each drug by UV–vis absorption. Ibu was analyzed at 230 nm, Lor at 250 nm, Rit at 239 nm, and Que at 370 nm. For dissolution experiments, aliquots were centrifuged at 13,000g for 10 min and the supernatant analyzed using UV/vis spectroscopy to determine drug concentration. Dissolution profiles for each drug/polymer formulation and for crystalline drugs are presented as concentration of drug in solution vs time (h).

Clarithromycin quantification was performed by HPLC-DAD. The HPLC system was an Agilent 1200 series consisting of a quaternary pump, online degasser, autosampler, and Agilent Chemstation LC 3D software. Chromatography was conducted in reversed phase mode using an Eclipse XDB-C18 column (4.6 × 150 mm internal diameter, particle size 5 μm). The mobile phase consisted of 60% acetonitrile and 40% pH 5.5 potassium phosphate buffer. Potassium phosphate monobasic (9.11 g) was dissolved in 1 L of water, 2 mL of triethylamine was added, and the pH was adjusted to 5.5 with phosphoric acid. The flow rate was 0.5 mL/min, and column temperature was 45 °C. Detection was achieved using a diode array detector (DAD) at 210 nm. CLA retention time was approximately 3.9 min. For dissolution experiments, 0.5 mL aliquots were centrifuged at 13,000g for 10 min and the supernatant was filtered using a 0.45 μm pore size hydrophilic PTFE filter prior to analysis.

For maximum drug solution concentrations, the ASD sample (drug content of 25 mg) was dispersed in 25 mL of 0.05 M pH 6.8 phosphate buffer at 37 °C with magnetic stirring (200 rpm). The concentration of each drug in solution was

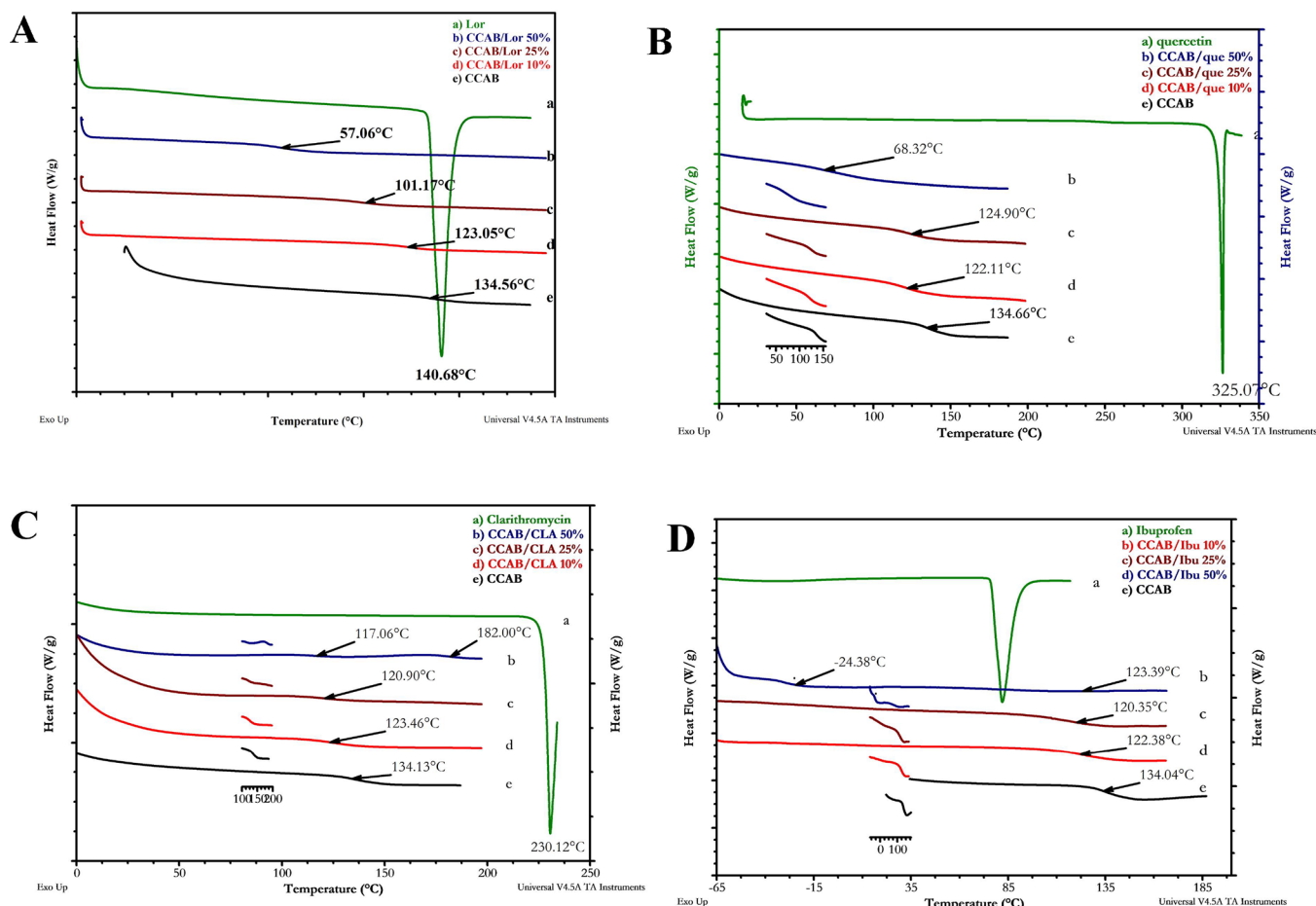


Figure 2. DSC thermograms of CCAB/drug dispersions vs CCAB and neat drug controls for (A) Lor, (B) Que, (C) Cla, and (D) Ibu.

measured by collecting 2.0 mL aliquots (0.5 mL for Cla) from the sample every 8 h (every hour for the first 2 h) until the drug concentration became constant (after 24–30 h). Each aliquot was centrifuged at 13,000g for 10 min, and then drug concentration in the supernatant was measured by UV-vis spectroscopy or HPLC-DAD.

2.9. In Vitro Drug Release. Dissolution of the drug from the CCAB matrix was compared to that of the crystalline drug using two experimental conditions. These dissolution experiments were performed using 250 mL jacketed flasks maintained at 37 °C. Release studies with pure drugs and ASDs were performed with initial amounts of drug as follows: Ibu 10 mg, Lor 5 mg, Que 5 mg, Rit 5 mg, and Cla 10 mg. Nonsink conditions were utilized in order to measure each formulation's effectiveness at obtaining and maintaining supersaturated drug concentrations. One-way analysis of variance (ANOVA) at the 95% confidence level was also used to compare the final drug concentrations, from individual dispersions and neat drugs, resulting from dissolution experiments.

2.9.1. Dissolution Experiment 1: Evaluation of Drug Release Profile from ASDs at pH 6.8. Drug/polymer samples were dispersed in 0.05 M pH 6.8 buffer (100 mL) and continuously magnetically stirred (37 °C and 200 rpm). Aliquots (2.0 or 0.5 mL for Cla) were withdrawn from the suspension every 0.5 h (during the first 2 h) and then every hour for a total of 8 h. Fresh phosphate buffer (2.0 or 0.5 mL)

was added to maintain constant volume after each aliquot was taken.

2.9.2. Dissolution Experiment 2: Evaluation of Drug Release at pH 1.2 Followed by pH 6.8. This experiment was designed to mimic pH changes during passage through the gastrointestinal (GI) tract and evaluate the effect of low pH (stomach pH) during the first 2 h on the dissolution of the drug from the ASDs. Formulations were first dispersed in 75 mL pH 1.2 HCl buffer solution for 2 h while being magnetically stirred at 200 rpm, with temperature maintained at 37 °C. Aliquots were withdrawn every 0.5 h for 2 h and centrifuged at 13,000g for 10 min, and the supernatant was assayed using UV-vis spectroscopy for drug concentration (reference calibration curve). To maintain constant volume, an equal volume of the appropriate buffer was replenished after removal of each aliquot. After 2 h, 25 mL of 0.05 M potassium phosphate buffer (pH 6.8) was added to the flask and the pH of the dissolution medium was adjusted to 6.8 with 5N NaOH. The dissolution experiment was continued for 6 h at pH 6.8 with aliquots (2.0 mL) withdrawn every 0.5 h (for the first hour) and then every hour. For Cla, 0.5 mL aliquots were withdrawn every 0.5 h for 2 h and neutralized with NaOH 5 N (approximately 6.5 μL) prior to analysis by HPLC as described in experimental section 2.8.

3. RESULTS AND DISCUSSION

3.1. Characterization of Spray-Dried CCAB/Drug Dispersions.

The five structurally diverse drug actives Ibu,

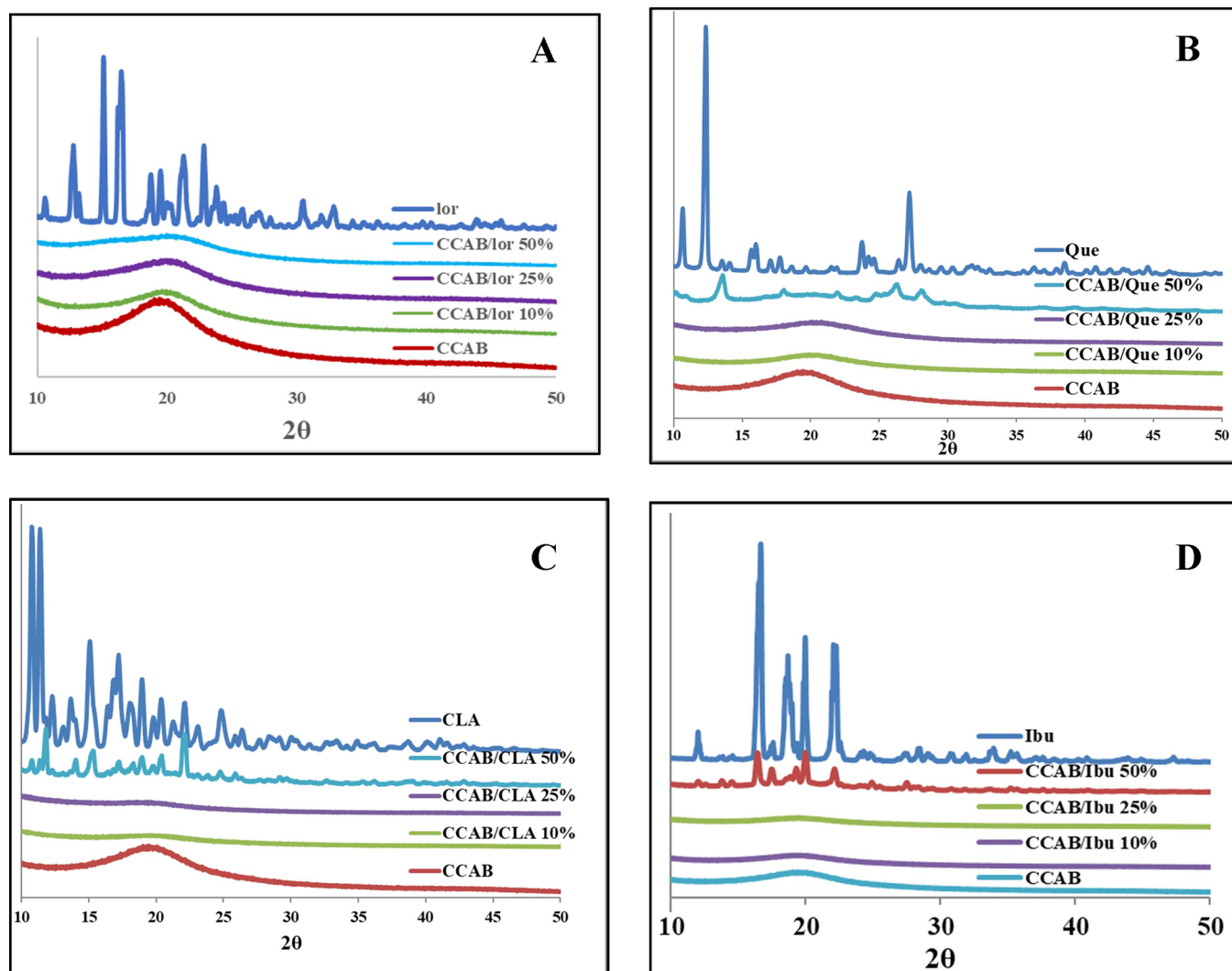


Figure 3. X-ray diffractograms for spray dried dispersions of (A) Lor, (B) Que, (C) Cla, and (D) Ibu versus CCAB and neat drug controls.

Lor, Que, Cla, and Rit were combined with CCAB to create dispersions by spray drying from solutions in methanol, acetonitrile, ethanol, methanol, and acetonitrile, respectively. Like many cellulose esters, CCAB has a high T_g (134 °C by DSC). This is promising for ASD formulation since a T_g value at least 40–50 °C above the highest possible ambient temperature (ca. 50 °C) is preferred for ASD, in order to provide a margin sufficient to overcome the plasticizing effects of both moisture and (potentially) drug, maintaining the formulation T_g above even the highest likely ambient temperatures under any humidity conditions. Spray-dried CCAB/drug dispersions and physical mixtures with 10% drug (Figure S2) were characterized as described below.

3.1.1. Differential Scanning Calorimetry (DSC). Lor, a crystalline antihistamine used to treat allergies, displays a sharp melting endotherm at 140 °C (DSC, Figure 2a). Solid dispersions of CCAB with 10, 25, and 50 wt % Lor showed only T_g endotherms, with no evidence of Lor crystallization or melting. The observed T_g values were lower than that of neat CCAB and decreased with an increasing drug percentage. T_g values of spray-dried CCAB/Lor blends agreed well with those calculated using the Fox–Flory equation^{42,43} (e.g., 124 °C observed, 122 °C calculated at 10% Lor), though some deviation was observed at 50% Lor (57 °C observed, 80 °C

calculated). The DSC thermogram of the CCAB/10% Lor physical mixture showed a melting endotherm at 133 °C (characteristic of pure Lor with T_m of 140 °C) as well as a glass transition at 150 °C (Figure S3). The flavonoid quercetin melts at a much higher temperature (325 °C, Figure 2b) than the other drugs studied. Que melting point (MP) lies above the onset temperature of CCAB decomposition; thus, the lack of Que MP by DSC cannot be used to indicate whether the dispersion is amorphous. CCAB/Que formulations did show single T_g values that decreased with increasing drug proportion (Figure 2b), consistent with amorphous dispersions. Cla is an aminomacrolide antibiotic that is prone to degradation under acidic conditions, made even more problematic by the fact that it has much higher solubility at acidic stomach pH than the neutral pH of the small intestine, both due to protonation of the Cla amine group.^{9,44} In order to circumvent Cla instability and provide more effective delivery systems, a number of different approaches have been utilized to enhance its delivery including formulation with cyclodextrins or lipids and ASDs with cellulose ω -carboxyalkanoates.⁹ DSC thermograms of 10 and 25% dispersions of clarithromycin in CCAB dispersion showed single T_g values (Figure 2c) that are only a few degrees below those predicted (Table S1), while 50% Cla formulations exhibited two distinct glass transitions (117 and 182 °C),

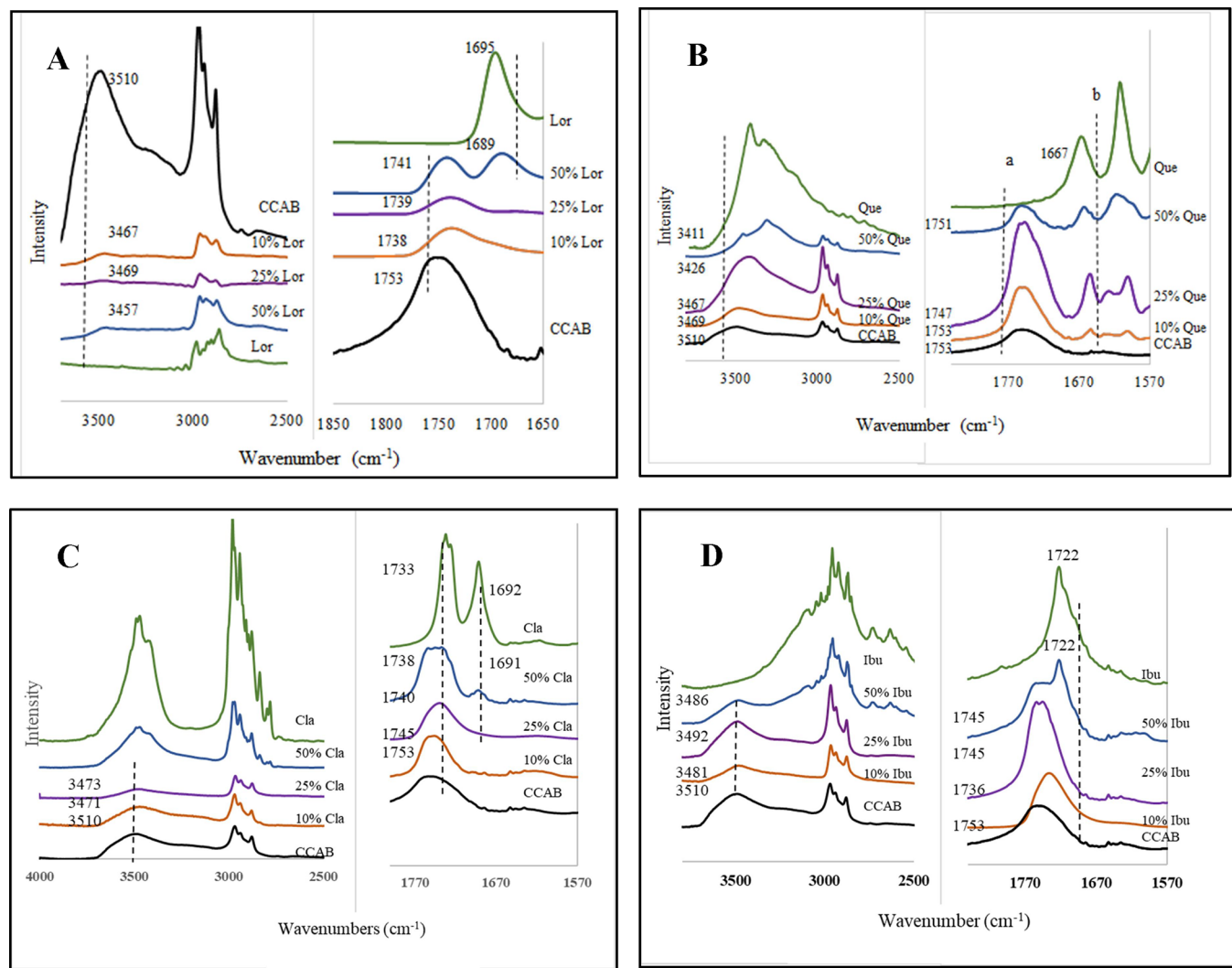


Figure 4. FTIR spectra for CCAB/drug dispersions vs CCAB and neat drug controls between 1650 and 1850 and 2500–3500 cm^{-1} for (A) Lor, (B) Que, (C) Cla, and (D) Ibu.

suggesting phase separation. The formulations were not heated beyond 200 $^{\circ}\text{C}$ to prevent degradation of CCAB. Lower drug-loading dispersions of CCAB with the anti-inflammatory drug ibuprofen also displayed single T_g values (DSC, Figure 2d), while the 50% Ibu dispersion indicated a second low temperature T_g ($-24\text{ }^{\circ}\text{C}$); pure Ibu exhibits T_g at $-41\text{ }^{\circ}\text{C}$. This indicates that at 50% Ibu there are separate phases, and even at 25% Ibu there is significant deviation from ideal, miscible behavior as indicated by T_g prediction by Fox–Flory eq (69 $^{\circ}\text{C}$) vs that measured (120 $^{\circ}\text{C}$). We have used Rit extensively in our laboratories as a model drug because of its poor aqueous solubility, importance in anti-HIV therapy⁴⁵ (and more recently, with lopinavir, in treatment of Covid-19 patients),⁴⁶ and relatively slow crystallization that facilitates comparison of ASD polymer effectiveness. Therefore, we chose to briefly examine the efficacy of CCAB as an ASD polymer for Rit. A 10% Rit: 90% CCAB powder, prepared by spray drying and analyzed by DSC, showed a single T_g at 123 $^{\circ}\text{C}$. FTIR and XRD analyses further confirmed the amorphous nature and miscibility of the dispersion. The resulting analyses can be found in the Supporting Information (Table S1, Figures S3, S4, S10 and S11).

3.1.2. X-ray Diffraction (XRD). XRD analysis (Figure 3a) of the Lor dispersions indicated only an amorphous halo, with no evidence of peaks from crystalline Lor. Therefore, evidence from both XRD and DSC supported the hypothesis that CCAB/Lor spray-dried blends are amorphous up to 50% drug. It was also evident from comparison of XRD and DSC data that spray-dried samples of CCAB/Lor were intimately mixed resulting in successful elimination of crystallinity, while physically mixed CCAB/Lor 10% retained Lor crystallinity (Figure S2). XRD diffractograms for Que dispersions showed that no sharp drug crystalline peaks were observed for the 10 and 25% drug dispersions, as they were for pure crystalline Que (Figure 3b), while the 50% dispersion did display evidence of significant residual Que crystallinity. For Cla, the 50% formulation showed crystalline peaks characteristic of the pure drug by XRD while no crystallinity was evident in the 10 and 25% Cla dispersions (Figure 3c). Comparative XRD data is also provided in Figure S2 for spray-dried and physically mixed 10% CLA dispersions. XRD analysis for Ibu dispersions (Figure 3d) also showed amorphous haloes for 10 and 25% dispersions of Ibu in CCAB, but significant Ibu crystallinity at 50% drug.

3.1.3. Fourier Transform Infrared (FTIR). FTIR spectra of the CCAB/Lor blends showed significant broadening and shifts to lower wavenumbers of the C=O peak for the 10 and 25% loratadine blends, indicative of increased hydrogen bonding interactions between the polymer and drug (Figure 4a). Significant broadening of the CCAB OH stretch could also be seen in the blends, with the peak shifting from 3510 cm^{-1} (pure CCAB) to 3467 and 3469 cm^{-1} for the 10 and 25% ASDs, respectively. For 50% Lor, two distinct peaks were seen in the C=O stretch region of the blend at wavenumbers characteristic of the drug (1689 cm^{-1}) and the polymer (1741 cm^{-1}). Since DSC and XRD showed no evidence of crystalline Lor in the 50% Lor blend, this may be a result of increasing Lor self-interaction with increased Lor content. The FTIR spectrum of the 50% CCAB/Que blend was more characteristic of that of the crystalline drug, especially between 2500 and 4000 cm^{-1} . In contrast, the 10% and 25% quercetin formulations showed increasing broadening and shift to lower wavenumbers of –OH stretch peaks at 3469 and 3467 cm^{-1} , respectively (Figure 4b), as quercetin content increased, supporting the XRD evidence that these are amorphous dispersions. These interactions result from the five H-bond donor (phenolic OH) groups on each quercetin molecule that are available to interact with the large number of C=O H-bond acceptor groups per CCAB molecule (Figure 1). FTIR spectra of CCAB/Cla also further supported Cla/CCAB miscibility at 10 and 25% drug, showing C=O peak shifts to lower wavenumbers (1740 and 1745 cm^{-1} compared to 1753 cm^{-1} for CCAB, Figure 4c) that indicate Cla-CCAB H-bonding. The notion of immiscibility of the 50% Ibu dispersion due to crystallinity is also supported by the FTIR spectra (Figure 4d). At 10% Ibu, there is a single carbonyl absorbance that appeared at wavenumbers between those of pure CCAB and pure ibuprofen. At 50% Ibu there were two distinct carbonyl peaks at 1722 and 1745 cm^{-1} , supporting significant phase separation at that high drug concentration.

3.2. Dissolution Testing and Solution Concentration Enhancement. We have calculated CCAB solubility in pH 6.8 buffer as 430 $\mu\text{g}/\text{mL}$, similar to the solubility of CAAdP^{24,25,34} known to be an effective ASD polymer but also on the hydrophobic end of the scale of effective polymers (Table 1). HPMCAS for example is an effective ASD polymer for many drugs, including in commercial formulations, and is more than an order of magnitude more soluble than CCAB. This could predict slower release from CCAB ASDs and could have implications for balancing polymer and drug dissolution rates. CCAB solubility in pH 1.2 buffer was

determined to be lower at 270 $\mu\text{g}/\text{mL}$, as expected for a carboxyl-containing polymer.

3.2.1. Maximum Drug Solution Concentrations and Drug Release at pH 6.8. In measuring drug release profiles, maximum possible drug concentrations were fixed to create the potential for supersaturation in pH 6.8 buffer solution (50 $\mu\text{g}/\text{mL}$ for Lor, Rit, and Que and 100 $\mu\text{g}/\text{mL}$ for Cla and Ibu), essential for comparison of amorphous solid dispersion polymers.^{26,30} Under supersaturating conditions *in vivo*, drug flux across the membrane of the intestinal cells is enhanced; thus, study of *in vitro* performance under supersaturating conditions is necessary to mimic and provide useful information about *in vivo* ASD polymer performance.⁵² Drug concentration was determined by UV-vis absorption or HPLC-DAD of the supernatants of samples centrifuged to remove particles and nanoparticles using appropriate standard curves. Drug release and solution concentration enhancement were highly drug-dependent, as described for individual drugs below.

Calculation of the maximum solution concentrations of crystalline Lor, Ibu, Cla, Rit, and Que shows that the achievable concentration of the drugs at pH 6.8 follows the order Ibu > Cla > Que > Lor > Rit (Figure 5) with Ibu reaching concentrations of 1.3 mg/mL and Rit showing concentrations of 1.6 $\mu\text{g}/\text{mL}$ in pH 6.8 buffer.

3.2.2. Loratadine. Study of Lor/CCAB ASD dissolution at pH 6.8 (Figure 6; 50 $\mu\text{g}/\text{mL}$ max concentration) showed no solubility enhancement for the hydrophobic Lor (log P value of 4.2⁵³) from CCAB ASD vs dissolution of crystalline drug. It is likely that relatively hydrophobic CCAB retards Lor release, while the drug also reduces the polymer release, thereby diminishing the advantage of ASD. Therefore, we explored whether utilizing a blended polymer matrix of CCAB and the hydrophilic, water-soluble ASD polymer PVP would enhance Lor release and maximum drug solution concentration. Pairwise polymer blends can provide synergistic and beneficial properties to polymer/drug formulation.^{8,14} A blend of CCAB/PVP (1:1, w:w) was prepared by spray drying and miscibility confirmed by FTIR and DSC (Table S1, Figures S4 and S6). Encouraged by the polymer miscibility, we prepared a spray-dried dispersion in the ratio 8:1:1 (CCAB: PVP: Lor). This dispersion was shown to be amorphous by XRD and displayed a single T_g by DSC (Figure S7 and Table S1). Characteristic shifts in the C=O and OH– stretch regions of the FTIR spectrum of 8:1:1 (CCAB:PVP:Lor) also support favorable interactions within the ternary ASD (Figure S6). Dissolution of the 10 wt % PVP dispersion in pH 6.8 buffer provided a 2-fold increase in Lor solution concentration vs neat drug or Lor formulated with CCAB only. It also afforded predicted faster drug release, achieving Lor supersaturation within 1 h and maintaining that supersaturation for the remainder of the experiment. Upon increasing PVP to 20 wt % (7:2:1 CCAB:PVP:Lor by weight), we observed even faster initial burst release, affording drug solution concentrations that were reasonably steady between 4 and 5 $\mu\text{g}/\text{mL}$ for the 8 h experiment duration. The 20% PVP formulations produced a final Lor concentration ~0.5 $\mu\text{g}/\text{mL}$ greater than that of the 10% PVP formulation. Dissolution of Lor from a PVP only formulation (Figure 6) showed rapid release within an hour with 36% of total drug released within that time. However, after 1 h, there was a drastic decrease in Lor concentration, indicating that PVP alone does not provide effective stabilization against recrystallization of the drug. The ternary

Table 1. Comparison of CCAB Physical Properties to Those of Other Common ASD Polymers

polymer	solubility ^a (mg/mL)	DS (CO_2H)	solubility parameter ($\text{MPa}^{1/2}$) ^b
PVP	>600 ⁷	N/A	28.4
HPMCAS	17.7 ⁹	0.40	22.4
CASub	3.0 ⁵⁰	0.65	22.6
CMCAB	0.8 ⁹	0.30	23.0
CCAB	0.43	0.28	24.4
CAAdp	0.3 ⁹	0.85	21.3

^aSolubility was determined in aqueous buffer (pH 6.8). ^bSolubility parameters (SP) calculated by the Fedors' method⁵¹ and described in the Supporting Information.

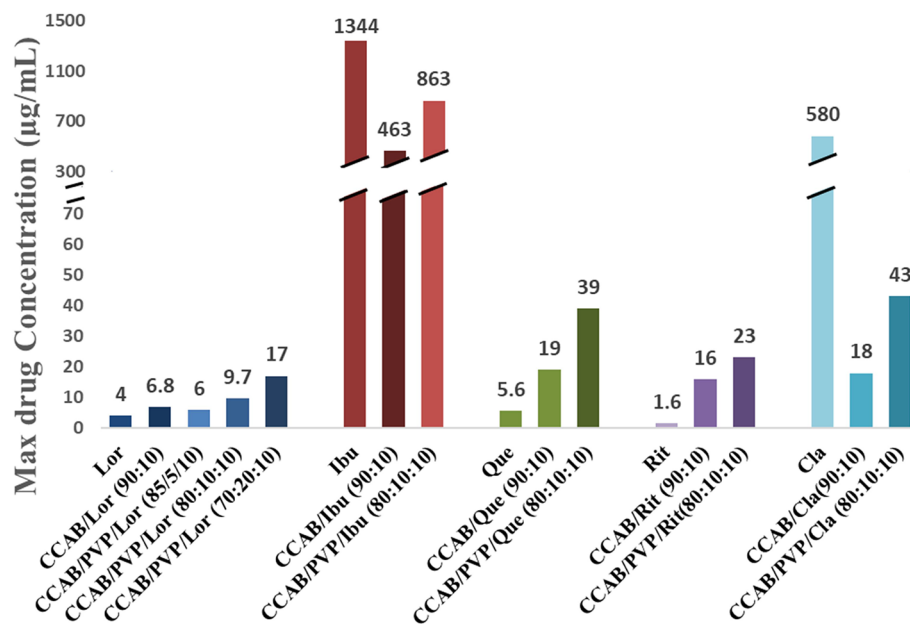


Figure 5. Maximum drug solution concentrations from ASDs and crystalline drugs in pH 6.8 phosphate buffer at 37 °C.

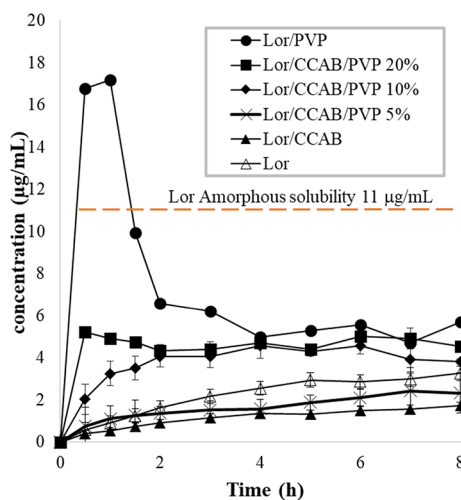


Figure 6. Dissolution profiles of 10% Lor with CCAB and ternary polymer/polymer/drug formulations with loratadine at pH 6.8. (Note: all formulations contain 10% Lor. Percent in key denotes % PVP in each ternary formulation).

formulation containing 20% PVP is thus synergistic, PVP providing faster Lor release, and CCAB providing more effective crystallization inhibition, thus sustaining high Lor concentration over the 8h period (Figure 6). Despite the solution enhancement provided, however, the highest resulting concentration of Lor from the ternary formulations was still $>2\times$ lower than its predicted amorphous solubility of 11 µg/mL.⁵⁴ The ternary formulation containing 20% PVP (Lor/CCAB/pvp 10/70/20) produced a significantly higher final concentration of loratadine ($p < 0.05$) compared to all binary Lor/CCAB dispersions and 10% ternary Lor/CCAB/PVP dispersions containing 5 and 10% PVP (Figure 6 and Table S2), indicating synergistic effects of the two polymers on loratadine release.

3.2.3. CCAB Solution Enhancement with Loratadine at Varying Concentrations. Recent studies have indicated the impact of the weight fraction of drug on achievable drug

concentrations from amorphous dispersions containing hydrophobic drug and poorly soluble (hydrophobic) polymers.⁵⁵ Loratadine was selected as a good candidate to assess the impact of increasing drug concentration on the achievable solution concentrations given its excellent miscibility with CCAB (up to 50 wt % drug). Over 8 h at pH 6.8, loratadine dispersions with CCAB showed increased solution concentrations as the quantity of drug in the formulation was increased. As seen in Figure 7 and Table S2, ASD formulations

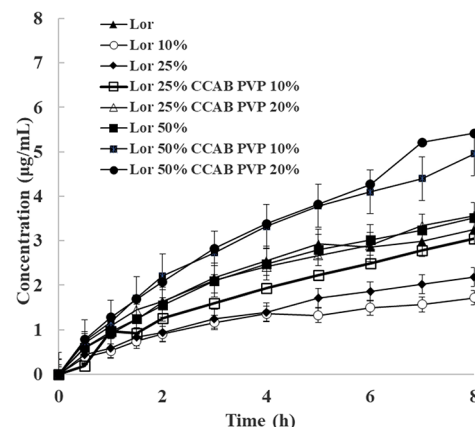


Figure 7. Lor dissolution profiles at pH 6.8 for Lor/CCAB formulations as the Lor concentration is increased in the binary blends. Note: 10, 25, and 50% indicate the wt % of Lor in the binary formulations.

containing 50% Lor showed a statistically significant 2-fold increase compared to 10 and 25 wt % dispersions. The 50% Lor formulation also reached drug concentrations similar to but not surpassing that of the crystalline drug. When 25 and 50 wt % Lor CCAB dispersions were also formulated with 10 or 20% PVP, a significant increase in solution concentration was achieved (Figure 7 and Table S2). The release was slow and controlled over the time period, despite being incomplete. The best performing formulations were Lor/CCAB/PVP

(10:70:20), Lor/CCAB/PVP (50:40:10), and Lor/CCAB/PVP (50:30:20), which provided significantly higher loratadine concentrations compared to the other formulations examined.

3.2.4. Ibuprofen. The anti-inflammatory drug Ibu is a 2-phenylpropionic acid that is quite soluble at small intestine pH, where it is ionized (Figure 8A), but has limited solubility in the

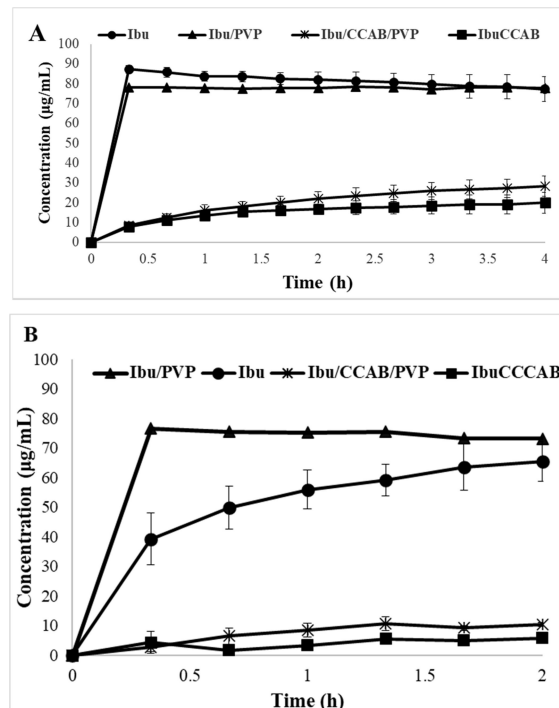


Figure 8. Dissolution profiles of CCAB/Ibu ASDs vs pure drug at pH 6.8 (A) and at pH 1.2 (B). All formulations contain 10% Ibu. 10% indicates wt % PVP.

fast-state stomach, where it is not (Figure 8B). The primary interest in incorporating Ibu into an ASD with a pH-responsive polymer like CCAB would be to create an Ibu formulation that released very little drug in the stomach, but generated supersaturation in the small intestine so that high bioavailability would be maintained, useful since Ibu can cause gastric irritation for some patients.⁵⁶ In pH 6.8 dissolution experiments (Figure 8A) with a maximum potential drug concentration of 100 µg/mL, Ibu itself dissolved rapidly, reaching about 90 µg/mL within 20 min. Release from 10% Ibu ASD in CCAB was much slower and controlled reaching 20% release in 4 h. Addition of 10% PVP to a formulation of CCAB and Ibu resulted in a slight increase (not statistically significant, $p > 0.05$) in Ibu concentration after 4 h (up to 28% drug release) while still maintaining slow and controlled release over the time period. Comparatively, the release of Ibu from a PVP only formulation was rapid, reaching ~80% within 20 min. To ascertain whether the binary formulation of CCAB and Ibu was capable of restricting Ibu release in the stomach, dissolution at pH 1.2 was monitored for 2 h (Figure 8B). Both the binary formulation of CCAB/Ibu and the ternary formulation of CCAB/Ibu/PVP exhibited very little Ibu release at stomach pH (4% and 9% respectively) while both pure drug and PVP only formulations exhibited higher Ibu concentrations over the time period. The difference in release for CCAB/Ibu and the ternary formulation of CCAB/Ibu/PVP at stomach pH was not statistically significant ($p > 0.05$). The

ability for CCAB, even in combination with the more water-soluble PVP, to restrict the release of Ibu at stomach pH has significant potential patient benefit.

3.2.5. Quercetin. The bioactive natural flavonoid quercetin has the lowest log P value (1.82) of the drugs we studied and is highly crystalline (melting point 314–316 °C),⁵⁷ resulting in very poor water solubility (measured as between 2⁵⁸ and 7⁵⁹ µg/mL); thus, it is an excellent candidate for ASD.^{7,60} The CCAB ASD containing 10% Que provided more than 3-fold maximum solution concentration increase in pH 6.8 buffer (Figure 5) vs crystalline Que, attaining a maximum of ca. 19 µg/mL. This was the largest increase in maximum drug concentration as a result of CCAB ASD of any of the drugs studied. In the pH 6.8 dissolution study (Figure 9), Que

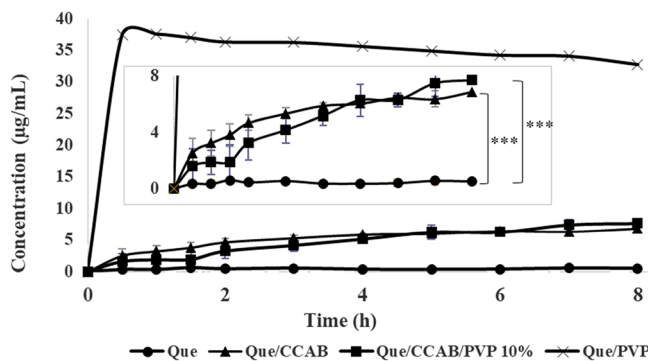


Figure 9. Que dissolution profiles at pH 6.8. All formulations contain 10% Que. “10%” in legend indicates wt % PVP. P values determined by one-way ANOVA: *** $p < 0.001$.

solution concentration was enhanced by more than 7-fold from this Que-CCAB ASD (6 µg/mL) vs Que only (<1 µg/mL for crystalline Que). Que dissolution from the CCAB ASD was significantly slower than that from crystalline Que, though eventually reaching much higher solution concentration (Figure 9). Since Que and CCAB are both quite hydrophobic, we expected that coformulation with the more hydrophilic PVP would improve Que release. Surprisingly, Que (10%) ternary ASD with CCAB (80%) and PVP (10%) instead provided Que dissolution rate and ultimate concentration very similar to those obtained from CCAB-only Que ASD. While there was significant increase in Que solution concentration from CCAB ASDs, only partial drug release was observed (~20%). It may be that the affinity of very hydrophobic Que for partly hydrophobic CCAB simply could not be overcome by PVP addition. As a comparison, Que dissolution from ASD in hydrophilic PVP alone occurs rapidly with ~75% Que release within the first 30 min, reaching a maximum of 37.4 µg/mL Que (Figure 9), dropping to 32 µg/mL after 8 h. Theoretical amorphous solubility is difficult to calculate due to the propensity of Que to melt with degradation. However, amorphous solubility calculated in the presence of PVP has been reported to reach at least 31.3 µg/mL in phosphate buffer at pH 6.8.⁶⁰ Studies have also revealed that structurally similar polyphenols such as resveratrol form soluble complexes in the presence of some polymers.⁶¹ Higher solution concentrations generated from ASDs could therefore in part be attributed to the presence of soluble drug-polymer complexes, supersaturation, or a combination of both effects.⁶¹ Therefore, the crystalline solubility of quercetin was also determined in the presence of PVP (20 mg/mL) or CCAB (20 mg/mL) in pH

6.8 phosphate buffer at 37 °C. The crystalline solubility in the absence of polymer was 5.6 $\mu\text{g}/\text{mL}$. The solubility in the presence of PVP was determined to be $84 \pm 9.3 \mu\text{g}/\text{mL}$, indicating a high likelihood that soluble complexes are being formed. In the presence of CCAB, Que crystalline solubility was $5.4 \pm 1.2 \mu\text{g}/\text{mL}$ showing no significant difference from its solubility in the absence of CCAB.

3.2.6. Clarithromycin. The antibiotic clarithromycin, despite its pH-sensitive solubility and propensity to degrade at acidic pH, displays a much greater thermodynamic solubility and hydrophilicity than most of the other APIs examined in the study. Dissolution of Cla at pH 6.8 indicated fast and complete release from hydrophilic PVP. On the other hand, release from a CCAB-only dispersion was delayed (beginning after 3 h) and incomplete, with only 2.5% of the drug released over the 8 h period (Figure 10A). CCAB hydrophobicity

recent results from Bapat et al.⁶² demonstrated a higher extent of insoluble complex formation for ionized cationic drug with anionic polymer HPMCAS. This in turn resulted in slower release of the cationic drug from the ASD. Similar ionic interactions/complexation between clarithromycin and CCAB could have an impact on the relative release rate of the drug even on switching to pH 6.8.

In order to better understand the influences at play in the loss of clarithromycin concentration at pH 1.2, the amount of clarithromycin remaining intact in a solution of drug only or a dispersion was quantified. 5 mg of clarithromycin (pure drug or equivalent mass in dispersion) was dispersed into 5 mL of pH 1.2 buffer at 37 °C with constant stirring at 200 rpm. After 2 h, the solution was neutralized with 65 μL of 5N NaOH and 5 mL of acetonitrile added to completely dissolve the contents. Each solution was quantitatively transferred to a 25 mL volumetric flask and made up to volume with the HPLC mobile phase. The concentration of clarithromycin in solution was quantified by HPLC (experimental section 2.8) and the % of clarithromycin remaining intact calculated. In the absence of polymer or from the PVP only dispersion, the amount of intact Cla was reduced to ~3% after 2 h while up to 100 or 95% remained in the CCAB only or ternary dispersion with CCAB/PVP, respectively (Figure S12). The confirmation of degradation versus recrystallization of Cla at pH 1.2 is consistent with previous work in our group.⁹ The high % of Cla remaining intact in the CCAB dispersions confirms the polymer's ability to protect clarithromycin from degradation at stomach pH; however, the inability to afford higher solution concentrations on switching to intestinal pH is a disadvantage of the formulations.

3.2.7. Ritonavir. Rit^{14,24,34} has been an important CYP-3A4 metabolic inhibitor, used in several anti-HIV and anti-Covid-19 commercial formulations, and we have designed a number of polysaccharide-based ASD polymers that significantly stabilize Rit against recrystallization. We therefore wished to compare the effectiveness of CCAB at enhancing the Rit solution concentration from ASD. A spray-dried dispersion (90 CCAB/10 Rit) was shown to be amorphous (XRD and DSC analyses, Figure S10 and Table S1). Upon pH 6.8 dissolution testing, this ASD provided a 3-fold increase in Rit solution concentration but achieved only 50% of the theoretical Rit amorphous solubility (20 $\mu\text{g}/\text{mL}$).³⁰ Further enhancement of Rit release from the otherwise hydrophobic formulation was achieved by incorporating 10% PVP in the ASD, affording Rit concentration of 14.7 $\mu\text{g}/\text{mL}$ after 8 h (>70% of theoretical amorphous solubility). It should be noted that Rit ASDs with several of our ASD-designed polymers, for example CASub, afford maximum Rit solution concentration without requiring added PVP.⁶³ Rit release from the CCAB ASD was also slower and more controlled for the duration of the experiment (Figure 11a). pH switch dissolution studies were also performed since higher Rit solubility at low pH is expected.⁶⁴ Its weakly basic thiazole groups have pK_a values of 1.8 and 2.6; thus, Rit exists as a dication at pH 1.2. However, at intestinal pH, Rit becomes un-ionized and its solubility quickly decreases. The pH switch experiment (Figure 11b) demonstrates that the hydrophobic CCAB matrix appears to protect Rit from dissolution at pH 1.2, while swelling of carboxylated CCAB provides a more effective release at pH 6.8, reaching the maximum Rit amorphous solubility within 2.5 h. Rit concentration even appears to increase further to 28 $\mu\text{g}/\text{mL}$ by the 8 h experimental terminus. Amorphous solubility values for

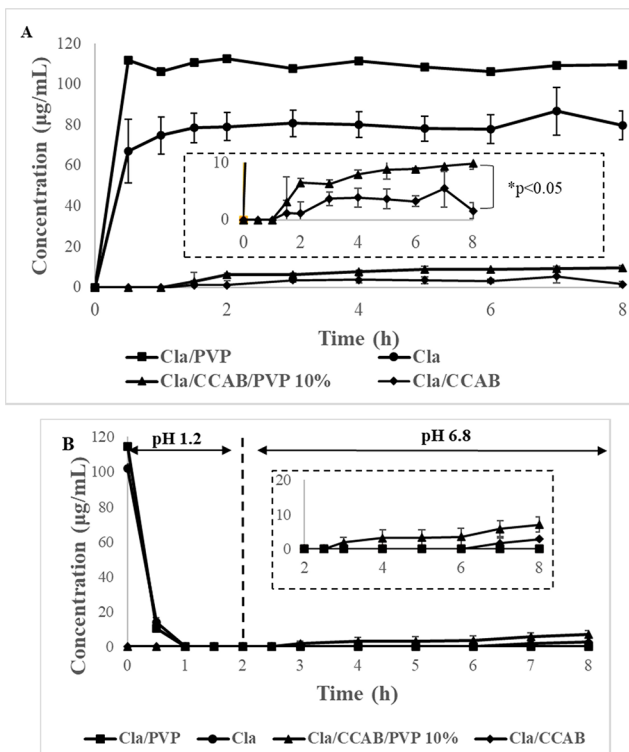


Figure 10. (A) Cla dissolution profiles at pH 6.8. (B) pH 1.2 for 2 h then pH 6.8 for 6 h (inset provides magnified view of drug concentration after 2 h). Note: all formulations contain 10% Cla. 10% indicates the wt % of PVP in ternary formulations. P values determined by one-way ANOVA: $*p < 0.05$.

appears to greatly impede achievable solution concentrations of Cla. Incorporation of 10% PVP into a ternary blend with CCAB and Cla provides a small increase in the level of dissolved Cla (only up to 10% drug release). Release from the ternary formulation was also delayed (beginning after 1.5 h) but increased steadily over the 8 h period to $\sim 10 \mu\text{g}/\text{mL}$. The concentration from the ternary dispersion was significantly different from the concentration from the binary dispersion ($p = 0.01$). In experiments mimicking the passage of the drug through the stomach then intestine (Figure 10B), a rapid decrease in drug concentration occurs in the initial 2 h at pH 1.2 for pure drug or from PVP only dispersion. Delivery of cationic drugs from ASDs of anionic polymers has been shown in the literature to be impacted by drug–polymer complex-

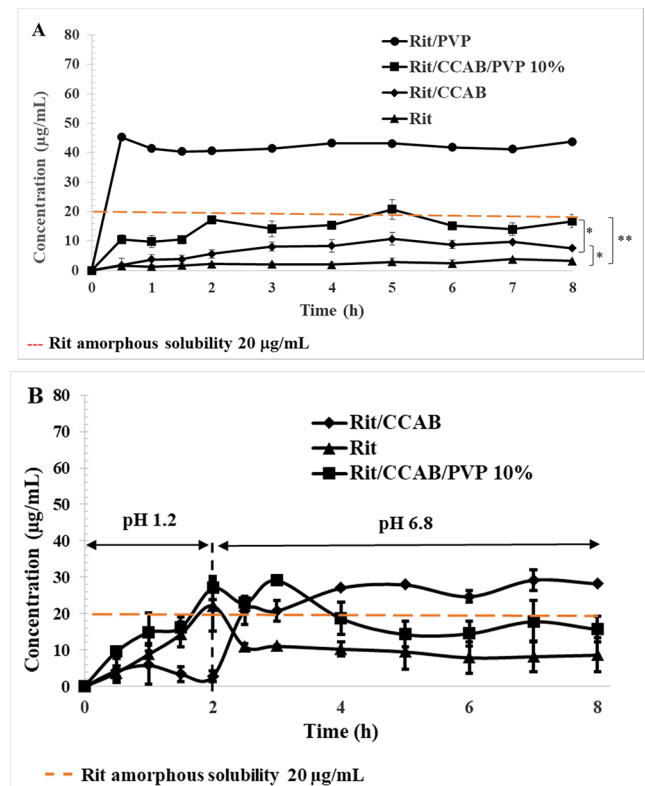


Figure 11. Rit dissolution profiles at (A) pH 6.8 and (B) pH 1.2 for 2 h and then pH 6.8 for 6 h. Note: all formulations contain 10% Rit. 10% indicates the wt % of PVP in ternary formulations. *P* values determined by one-way ANOVA: **p* < 0.05, ***p* < 0.01.

ritonavir have been reported up to 27 μg/mL (in 100 mM pH 6.8 phosphate buffer)⁶⁵ and thus reported values show some variability (20 to 27 μg/mL) depending on the ionic strength of the buffer. High apparent solution concentration can also be due to interference from formation of a separate ritonavir nanodroplet phase.^{53,66,67} Dissolution of Rit from ASD with PVP only is rapid at pH 6.8, with ~90% of drug released within 0.5 h. The ternary blend (80 CCAB/10 PVP/10 Rit) afforded higher Rit release at low pH, as expected with the soluble PVP, and afforded higher overall Rit release, but with some reduction in concentration over time at pH 6.8. Differences in Rit concentrations between the pH 6.8 dissolution experiments were statistically significant (*p* < 0.05), while differences in Rit concentration resulting from the various pH switch experiments were not.

4. CONCLUSIONS

CCAB is clearly effective at providing miscible, amorphous blends with a diverse array of otherwise highly crystalline drugs including Que, Lor, Ibu, Cla, and Rit. Amorphous dispersion in CCAB affords significant solubility enhancement for certain hydrophobic drugs, including Rit and Que. It is quite convenient to formulate CCAB/drug ASDs by spray drying due to the broad solvent solubility of CCAB. Some ASDs with extremely hydrophobic drugs, for example Lor, may provide more controlled, slower release of the drug but not significant solubility enhancement due to the hydrophobicity of CCAB. This issue can be mitigated in some cases, including for Lor, by adding a small percentage of water-soluble PVP, with which CCAB shows good miscibility. Such a strategy provided a 2-

fold increase in Lor solution concentration versus drug only (up to ~5 μg/mL). CCAB hydrophobicity and pH-responsiveness can be used to reduce exposure of drugs like Ibu and Cla to the stomach, thereby potentially reducing GI side effects or drug degradation, erasing issues of variability due to stomach pH, and enabling extended release formulations. The results from these experiments show that CCAB is a promising matrix polymer for amorphous solid dispersions. The carboxyl content of commercial CCAB (DS 0.28) is much lower than that of excellent ASD polymers such as cellulose acetate suberate (CASub, DS 0.85). Ionization of carboxyls is critical to drug release, polymer aqueous solubility (some polymer solubility is needed to afford stabilization of supersaturated drug solutions against recrystallization), and polymer–drug interaction that reduces the energy of amorphous drug and therefore the driving force for crystallization. The maximum DS(CO₂H) of a CCAB analog would of course be 1.0, and a CCAB analog with higher DS(CO₂H), perhaps matching that of CASub, would be predicted to be a much more broadly effective ASD polymer. Commercial CCAB is a reasonable choice for ASD of hydrophobic, crystalline drugs, potentially in combination with more hydrophilic polymers such as PVP. In some cases, it is likely to prove quite useful. It is not currently in any approved drug formulations, and therefore, toxicity testing and approvals would be needed; however, the polymer and its reasonable degradation products like acetic acid and butyric acid (endogenous and dietary, respectively) are likely to display very low toxicity. These results show the utility of CCAB itself and also provide a good example of the potential benefits of ternary amorphous formulation by pairwise polymer blending.

ASSOCIATED CONTENT

Supporting Information

The Supporting Information is available free of charge at <https://pubs.acs.org/doi/10.1021/acs.molpharmaceut.4c00493>.

¹H NMR for CCAB, solubility parameters calculation, XRD diffractograms of physical mixtures, loratadine blends and ritonavir blends, comparison of *T*_g values for ASDs, intact clarithromycin % after 2 h at pH 1.2, analysis of variance (ANOVA) for drug concentration from Lor dispersions (DOCX)

AUTHOR INFORMATION

Corresponding Author

Joyann A. Marks — *Macromolecules Innovation Institute, Department of Sustainable Biomaterials, College of Natural Resources and Environment, Virginia Tech, Blacksburg, Virginia 24061, United States; Department of Chemistry, University of the West Indies, Kingston JMAW15, Jamaica; orcid.org/0000-0001-9062-3532; Email: joyannam@vt.edu*

Authors

Brittany L. B. Nichols — *Department of Chemistry, College of Science, Virginia Tech, Blacksburg, Virginia 24061, United States*
Laura I. Mosquera-Giraldo — *Department of Industrial and Physical Pharmacy, College of Pharmacy, Purdue University, West Lafayette, Indiana 47907, United States*

Sara T. Yazdi — *Macromolecules Innovation Institute, Department of Sustainable Biomaterials, College of Natural Resources and Environment, Virginia Tech, Blacksburg, Virginia 24061, United States*

Lynne S. Taylor — *Department of Industrial and Physical Pharmacy, College of Pharmacy, Purdue University, West Lafayette, Indiana 47907, United States;  orcid.org/0000-0002-4568-6021*

Kevin J. Edgar — *Macromolecules Innovation Institute, Department of Sustainable Biomaterials, College of Natural Resources and Environment, Virginia Tech, Blacksburg, Virginia 24061, United States;  orcid.org/0000-0002-9459-9477*

Complete contact information is available at:
<https://pubs.acs.org/10.1021/acs.molpharmaceut.4c00493>

Notes

The authors declare no competing financial interest.

ACKNOWLEDGMENTS

The authors wish to thank Eastman Chemical Company for their kind donation of CCAB. We are grateful to the VT Macromolecules Innovation Institute, Department of Sustainable Biomaterials — Virginia Tech and the University of the West Indies, Mona for their support, and to VT ICTAS for their material and facilities support. We thank the U.S. National Science Foundation for partial support of this work (DMR-2204996, KE). We also wish to thank Dr. Ann Norris (Department of Sustainable Biomaterials, Virginia Tech), Jeffrey Thompson (Department of Chemistry, Virginia Tech) and Dr. Jing Zhao (Department of Geosciences, Virginia Tech) for their assistance in obtaining XRD analyses.

REFERENCES

- (1) Liechty, W. B.; Kryscio, D. R.; Slaughter, B. V.; Peppas, N. A. Polymers for Drug Delivery Systems. *Annu. Rev. Chem. Biomol. Eng.* **2010**, *1*, 149.
- (2) Uhrich, K. E.; Cannizzaro, S. M.; Langer, R. S.; Shakesheff, K. M. Polymeric Systems for Controlled Drug Release. *Chem. Rev.* **1999**, *99* (11), 3181–3198.
- (3) Pillai, O.; Panchagnula, R. Polymers in Drug Delivery. *Curr. Opin. Chem. Biol.* **2001**, *5* (4), 447–451.
- (4) Edgar, K. J. Cellulose Esters in Drug Delivery. *Cellulose* **2007**, *14* (1), 49–64.
- (5) Edgar, K. J.; Buchanan, C. M.; Debenham, J. S.; Rundquist, P. A.; Seiler, B. D.; Shelton, M. C.; Tindall, D. Advances in Cellulose Ester Performance and Application. *Prog. Polym. Sci.* **2001**, *26* (9), 1605–1688.
- (6) Kosaka, P. M.; Kawano, Y.; Salvadori, M. C.; Petri, D. F. S. Characterization of Ultrathin Films of Cellulose Esters. *Cellulose* **2005**, *12* (4), 351–359.
- (7) Li, B.; Konecke, S.; Harich, K.; Wegiel, L.; Taylor, L. S.; Edgar, K. J. Solid Dispersion of Quercetin in Cellulose Derivative Matrices Influences Both Solubility and Stability. *Carbohydr. Polym.* **2013**, *92* (2), 2033–2040.
- (8) Marks, J. A.; Wegiel, L. A.; Taylor, L. S.; Edgar, K. J. Pairwise Polymer Blends for Oral Drug Delivery. *J. Pharm. Sci.* **2014**, *103* (9), 2871–2883.
- (9) Pereira, J. M.; Mejia-Ariza, R.; Ilevbare, G. A.; McGettigan, H. E.; Sriranganathan, N.; Taylor, L. S.; Davis, R. M.; Edgar, K. J. Interplay of Degradation, Dissolution and Stabilization of Clarithromycin and Its Amorphous Solid Dispersions. *Mol. Pharmaceutics* **2013**, *10* (12), 4640–4653.
- (10) Li, B.; Wegiel, L. A.; Taylor, L. S.; Edgar, K. J. Stability and Solution Concentration Enhancement of Resveratrol by Solid Dispersion in Cellulose Derivative Matrices. *Cellulose* **2013**, *20* (3), 1249–1260.
- (11) Wang, P.; Tao, B. Y. Synthesis and Characterization of Long-chain Fatty Acid Cellulose Ester (FACE). *J. Appl. Polym. Sci.* **1994**, *52* (6), 755–761.
- (12) Mohanty, A. K.; Wibowo, A.; Misra, M.; Drzal, L. T. Development of Renewable Resource-Based Cellulose Acetate Bioplastic: Effect of Process Engineering on the Performance of Cellulosic Plastics. *Polym. Eng. Sci.* **2003**, *43* (5), 1151–1161.
- (13) Klemm, D.; Heublein, B.; Fink, H.-P.; Bohn, A. Cellulose: Fascinating Biopolymer and Sustainable Raw Material. *Angew. Chem., Int. Ed.* **2005**, *44* (22), 3358–3393.
- (14) Ilevbare, G. A.; Liu, H.; Edgar, K. J.; Taylor, L. S. Effect of Binary Additive Combinations on Solution Crystal Growth of the Poorly Water-Soluble Drug. *Ritonavir. Cryst. Growth Des.* **2012**, *12* (12), 6050–6060.
- (15) Wegiel, L. A.; Mauer, L. J.; Edgar, K. J.; Taylor, L. S. Crystallization of Amorphous Solid Dispersions of Resveratrol during Preparation and Storage—Impact of Different Polymers. *J. Pharm. Sci.* **2013**, *102* (17).
- (16) Miller, J. M.; Beig, A.; Carr, R. A.; Spence, J. K.; Dahan, A. A Win–Win Solution in Oral Delivery of Lipophilic Drugs: Supersaturation via Amorphous Solid Dispersions Increases Apparent Solubility without Sacrifice of Intestinal Membrane Permeability. *Mol. Pharmaceutics* **2012**, *9* (7), 2009–2016.
- (17) Curatolo, W.; Nightingale, J. A.; Herbig, S. M. Utility of Hydroxypropylmethylcellulose Acetate Succinate (HPMCAS) for Initiation and Maintenance of Drug Supersaturation in the GI Milieu. *Pharm. Res.* **2009**, *26* (6), 1419–1431.
- (18) Shah, N.; Iyer, R. M.; Mair, H.-J.; Choi, D.; Tian, H.; Diodone, R.; Fahnrich, K.; Pabst-Ravot, A.; Tang, K.; Scheubel, E.; Grippo, J. F.; Moreira, S. A.; Go, Z.; Mouskountakis, J.; Louie, T.; Ibrahim, P. N.; Sandhu, H.; Rubia, L.; Chokshi, H.; Singhal, D.; Malick, W. Improved Human Bioavailability of Vemurafenib, a Practically Insoluble Drug, Using an Amorphous Polymer-Stabilized Solid Dispersion Prepared by a Solvent-Controlled Coprecipitation Process. *J. Pharm. Sci.* **2013**, *102* (3), 967–981.
- (19) Tanno, F.; Nishiyama, Y.; Kokubo, H.; Obara, S. Evaluation of Hypromellose Acetate Succinate (HPMCAS) as a Carrier in Solid Dispersions. *Drug Dev. Ind. Pharm.* **2004**, *30* (1), 9–17.
- (20) Trasi, N. S.; Taylor, L. S. Effect of Polymers on Nucleation and Crystal Growth of Amorphous Acetaminophen. *CrystEngComm* **2012**, *14* (16), 5188–5197.
- (21) Posey-Dowty, J. D.; Watterson, T. L.; Wilson, A. K.; Edgar, K. J.; Shelton, M. C.; Lingerfelt, L. R. Zero-Order Release Formulations Using a Novel Cellulose Ester. *Cellulose* **2007**, *14* (1), 73–83.
- (22) Shelton, M. C.; Posey-Dowty, J. D.; Lingerfelt, L.; Kirk, S. K.; Klein, S.; Edgar, K. J. Enhanced Dissolution of Poorly Soluble Drugs from Solid Dispersions in Carboxymethylcellulose Acetate Butyrate Matrices. In *Polysaccharide Materials: Performance by Design*; American Chemical Society, 2009; Vol. 1017, pp 93–113.
- (23) Posey-Dowty, J.; Watterson, T.; Edgar, K.; Kirk, S.; Welty, M.; Yuan, J.; Shelton, M.; Lingerfelt, L.; Wilson, A. *Carboxyalkyl Cellulose Esters for Sustained Delivery of Pharmaceutically Active Substances*, 2007.
- (24) Ilevbare, G.; Liu, H.; Edgar, K. J.; Taylor, L. S. Inhibition of Solution Crystal Growth of Ritonavir by Cellulose Polymers—Factors Influencing Polymer Effectiveness. *CrystEngComm* **2012**, *14* (20), 6503–6514.
- (25) Liu, H.; Ilevbare, G. A.; Cherniawski, B. P.; Ritchie, E. T.; Taylor, L. S.; Edgar, K. J. Synthesis and Structure–Property Evaluation of Cellulose ω -Carboxyesters for Amorphous Solid Dispersions. *Carbohydr. Polym.* **2014**, *100* (0), 116–125.
- (26) Ilevbare, G. A.; Liu, H.; Edgar, K. J.; Taylor, L. S. Impact of Polymers on Crystal Growth Rate of Structurally Diverse Compounds from Aqueous Solution. *Mol. Pharmaceutics* **2013**, *10* (6), 2381–2393.
- (27) Dong, Y.; Mosquera-Giraldo, L. I.; Taylor, L. S.; Edgar, K. J. Amphiphilic Cellulose Ethers Designed for Amorphous Solid Dispersion via Olefin Cross-Metathesis. *Biomacromolecules* **2016**, *17* (2), 454–465.

(28) Dong, Y.; Mosquera-Giraldo, L. I.; Troutman, J.; Skogstad, B.; Taylor, L. S.; Edgar, K. J. Amphiphilic Hydroxyalkyl Cellulose Derivatives for Amorphous Solid Dispersion Prepared by Olefin Cross-Metathesis. *Polym. Chem.* **2016**, *7* (30), 4953–4963.

(29) Dong, Y.; Matson, J. B.; Edgar, K. J. Olefin Cross-Metathesis in Polymer and Polysaccharide Chemistry: A Review. *Biomacromolecules* **2017**, *12*, 1661–1676.

(30) Ilevbare, G. A.; Liu, H.; Edgar, K. J.; Taylor, L. S. Maintaining Supersaturation in Aqueous Drug Solutions: Impact of Different Polymers on Induction Times. *Cryst. Growth Des.* **2013**, *13* (2), 740–751.

(31) Zecevic, D. E.; Meier, R.; Daniels, R.; Wagner, K.-G. Site Specific Solubility Improvement Using Solid Dispersions of HPMC-AS/HPC SSL – Mixtures. *Eur. J. Pharm. Biopharm.* **2014**, *87* (2), 264–270.

(32) Van den Mooter, G. The Use of Amorphous Solid Dispersions: A Formulation Strategy to Overcome Poor Solubility and Dissolution Rate. *Drug Discovery Today: Technologies* **2012**, *9*, e79–e85.

(33) Liu, H.; Taylor, L. S.; Edgar, K. J. The Role of Polymers in Oral Bioavailability Enhancement. A Review. *Polymer (Guildf)* **2015**, *77*, 399–415.

(34) Ilevbare, G. A.; Liu, H.; Edgar, K. J.; Taylor, L. S. Understanding Polymer Properties Important for Crystal Growth Inhibition—Impact of Chemically Diverse Polymers on Solution Crystal Growth of Ritonavir. *Cryst. Growth Des.* **2012**, *12* (6), 3133–3143.

(35) Buchanan, C. M.; Buchanan, N. L.; Carty, S. N.; Kuo, C. M.; Lambert, J. L.; Malcolm, M. O.; Posey-Dowty, J. D.; Watterson, T. L.; Wood, M. D.; Lindblad, M. S.; Malcolm, M. O.; Lindblad, M. S. *Cellulose Interpolymers and Method of Oxidation*, 2013.

(36) Zhang, Y.; Chen, J.; Zhang, G.; Lu, J.; Yan, H.; Liu, K. Sustained Release of Ibuprofen from Polymeric Micelles with a High Loading Capacity of Ibuprofen in Media Simulating Gastrointestinal Tract Fluids. *React. Funct. Polym.* **2012**, *72* (6), 359–364.

(37) Vueba, M. L.; Veiga, F.; Sousa, J. J.; Pina, M. E. Compatibility Studies between Ibuprofen or Ketoprofen with Cellulose Ether Polymer Mixtures Using Thermal Analysis. *Drug Dev. Ind. Pharm.* **2005**, *31* (10), 943–949.

(38) Rivera-Leyva, J. C.; García-Flores, M.; Valladares-Méndez, A.; Orozco-Castellanos, L. M.; Martínez-Alfaro, M. Comparative Studies on the Dissolution Profiles of Oral Ibuprofen Suspension and Commercial Tablets Using Biopharmaceutical Classification System Criteria. *Indian J. Pharm. Sci.* **2012**, *74* (4), 312–318.

(39) Zeeshan, F.; Bukhari, N. I. Development and Evaluation of a Novel Modified-Release Pellet-Based Tablet System for the Delivery of Loratadine and Pseudoephedrine Hydrochloride as Model Drugs. *AAPS PharmSciTech* **2010**, *11* (2), 910–916.

(40) Bureau, G.; Longpré, F.; Martinoli, M. Resveratrol and Quercetin, Two Natural Polyphenols, Reduce Apoptotic Neuronal Cell Death Induced by Neuroinflammation. *J. Neurosci Res.* **2008**, *86* (2), 403–410.

(41) Arca, H. Ç.; Mosquera-Giraldo, L. I.; Dahal, D.; Taylor, L. S.; Edgar, K. J. Multidrug, Anti-HIV Amorphous Solid Dispersions: Nature and Mechanisms of Impacts of Drugs on Each Other's Solution Concentrations. *ACS Publications* **2017**, *14* (11), 3617–3627.

(42) Fox, T. G. Influence of Diluent and of Copolymer Composition on the Glass Temperature of a Polymer System. *Bull. Am. Phys. Soc.* **1956**, *1* (123), 22060–26218.

(43) Nyamweya, N.; Hoag, S. W. Assessment of Polymer-Polymer Interactions in Blends of HPMC and Film Forming Polymers by Modulated Temperature Differential Scanning Calorimetry. *Pharm. Res.* **2000**, *17* (5), 625–631.

(44) Ōmura, S. *Macrolide Antibiotics: Chemistry, Biology, and Practice*; Academic Press, 2002.

(45) Hull, M. W.; Montaner, J. S. G. Ritonavir-Boosted Protease Inhibitors in HIV Therapy. *Ann. Med.* **2011**, *43* (5), 375–388.

(46) Cao, B.; Wang, Y.; Wen, D.; Liu, W.; Wang, J.; Fan, G.; Ruan, L.; Song, B.; Cai, Y.; Wei, M.; Li, X.; Xia, J.; Chen, N.; Xiang, J.; Yu, T.; Bai, T.; Xie, X.; Zhang, L.; Li, C.; Yuan, Y.; Chen, H.; Li, H.; Huang, H.; Tu, S.; Gong, F.; Liu, Y.; Wei, Y.; Dong, C.; Zhou, F.; Gu, X.; Xu, J.; Liu, Z.; Zhang, Y.; Li, H.; Shang, L.; Wang, K.; Li, K.; Zhou, X.; Dong, X.; Qu, Z.; Lu, S.; Hu, X.; Ruan, S.; Luo, S.; Wu, J.; Peng, L.; Cheng, F.; Pan, L.; Zou, J.; Jia, C.; Wang, J.; Liu, X.; Wang, S.; Wu, X.; Ge, Q.; He, J.; Zhan, H.; Qiu, F.; Guo, L.; Huang, C.; Jaki, T.; Hayden, F. G.; Horby, P. W.; Zhang, D.; Wang, C. A Trial of Lopinavir–Ritonavir in Adults Hospitalized with Severe Covid-19. *N. Engl. J. Med.* **2020**, *382* (19), 1787–1799.

(47) Friesen, D. T.; Shanker, R.; Crew, M.; Smithey, D. T.; Curatolo, W. J.; Nightingale, J. A. S. Hydroxypropyl Methylcellulose Acetate Succinate-Based Spray-Dried Dispersions: An Overview. *Mol. Pharmaceutics* **2008**, *5* (6), 1003–1019.

(48) Hu, Q.; Choi, D. S.; Chokshi, H.; Shah, N.; Sandhu, H. Highly Efficient Miniaturized Coprecipitation Screening (MiCoS) for Amorphous Solid Dispersion Formulation Development. *Int. J. Pharm.* **2013**, *450*, 53–62.

(49) Dow Chemical Co. *AFFINOSOLTM HPMCAS for Spray-Dried Dispersion (SDD) Solving the Insoluble with Dow*; 2014.

(50) Arca, H. Ç.; Mosquera-Giraldo, L. I.; Pereira, J. M.; Sriranganathan, N.; Taylor, L. S.; Edgar, K. J. Rifampin Stability and Solution Concentration Enhancement Through Amorphous Solid Dispersion in Cellulose ω -Carboxyalkanoate Matrices. *J. Pharm. Sci.* **2018**, *107* (1), 127–138.

(51) Fedors, R. F. A Method for Estimating Both the Solubility Parameters and Molar Volumes of Liquids. *Polym. Eng. Sci.* **1974**, *14* (2), 147–154.

(52) Sun, D. D.; Wen, H.; Taylor, L. S. Non-Sink Dissolution Conditions for Predicting Product Quality and *in vivo* Performance of Supersaturating Drug Delivery Systems. *J. Pharm. Sci.* **2016**, *105* (9), 2477–2488.

(53) Ilevbare, G. A.; Taylor, L. S. Liquid–Liquid Phase Separation in Highly Supersaturated Aqueous Solutions of Poorly Water-Soluble Drugs: Implications for Solubility Enhancing Formulations. *Cryst. Growth Des.* **2013**, *13* (4), 1497–1509.

(54) Hsieh, Y.-L.; Ilevbare, G. A.; Van Eerdenbrugh, B.; Box, K. J.; Sanchez-Felix, M. V.; Taylor, L. S. PH-Induced Precipitation Behavior of Weakly Basic Compounds: Determination of Extent and Duration of Supersaturation Using Potentiometric Titration and Correlation to Solid State Properties. *Pharm. Res.* **2012**, *29* (10), 2738–2753.

(55) Li, N.; Taylor, L. S. Tailoring Supersaturation from Amorphous Solid Dispersions. *J. Controlled Release* **2018**, *279*, 114–125.

(56) Semble, E. L.; Wu, W. C. *Antiinflammatory Drugs and Gastric Mucosal Damage*. In *Seminars in arthritis and rheumatism*; Elsevier, 1987; Vol. 16, pp 271–286.

(57) Wattenberg, L. W.; Leong, J. L.; Galbraith, A. R. Induction of Increased Benzpyrene Hydroxylase Activity by Flavones and Related Compounds. *Cancer Res.* **1968**, *28*, 934.

(58) Srinivas, K.; King, J. W.; Howard, L. R.; Monrad, J. K. Solubility and Solution Thermodynamic Properties of Quercetin and Quercetin Dihydrate in Subcritical Water. *J. Food Eng.* **2010**, *100*, 208.

(59) Lauro, M. R.; Torre, M. L.; Maggi, L.; De Simone, F.; Conte, U.; Aquino, R. P. Fast-and Slow-Release Tablets for Oral Administration of Flavonoids: Rutin and Quercetin. *Drug Dev. Ind. Pharm.* **2002**, *28* (4), 371–379.

(60) Gilley, A. D.; Arca, H. C.; Nichols, B. L. B.; Mosquera-Giraldo, L. I.; Taylor, L. S.; Edgar, K. J.; Neilson, A. P. Novel Cellulose-Based Amorphous Solid Dispersions Enhance Quercetin Solution Concentrations *in vitro*. *Carbohydr. Polym.* **2017**, *157*, 86–93.

(61) Wegiel, L. A.; Mosquera-Giraldo, L. I.; Mauer, L. J.; Edgar, K. J.; Taylor, L. S. Phase Behavior of Resveratrol Solid Dispersions Upon Addition to Aqueous Media. *Pharm. Res.* **2015**, *32* (10), 3324–3337.

(62) Bapat, P.; Paul, S.; Tseng, Y.-C.; Taylor, L. S. Interplay of Drug–Polymer Interactions and Release Performance for HPMCAS-Based Amorphous Solid Dispersions. *Mol. Pharmaceutics* **2024**, *21* (3), 1466–1478.

(63) Liu, H.; Ilevbare, G. A.; Cherniawski, B. P.; Ritchie, E. T.; Taylor, L. S.; Edgar, K. J. Synthesis and Structure–Property

Evaluation of Cellulose ω -Carboxyesters for Amorphous Solid Dispersions. *Carbohydr. Polym.* **2014**, *100* (0), 116–125.

(64) Law, D.; Krill, S. L.; Schmitt, E. A.; Fort, J. J.; Qiu, Y.; Wang, W.; Porter, W. R. Physicochemical Considerations in the Preparation of Amorphous Ritonavir–Poly (Ethylene Glycol) 8000 Solid Dispersions. *J. Pharm. Sci.* **2001**, *90* (8), 1015–1025.

(65) Purohit, H. S.; Taylor, L. S. Phase Behavior of Ritonavir Amorphous Solid Dispersions during Hydration and Dissolution. *Pharm. Res.* **2017**, *34* (12), 2842–2861.

(66) Ilevbare, G. A.; Liu, H.; Pereira, J.; Edgar, K. J.; Taylor, L. S. Influence of Additives on the Properties of Nanodroplets Formed in Highly Supersaturated Aqueous Solutions of Ritonavir. *ACS Publications* **2013**, *10* (9), 3392–3403.

(67) Indulkar, A. S.; Waters, J. E.; Mo, H.; Gao, Y.; Raina, S. A.; Zhang, G. G. Z.; Taylor, L. S. Origin of Nanodroplet Formation Upon Dissolution of an Amorphous Solid Dispersion: A Mechanistic Isotope Scrambling Study. *J. Pharm. Sci.* **2017**, *106* (8), 1998–2008.

■ NOTE ADDED AFTER ASAP PUBLICATION

This paper was published ASAP on August 1, 2024, with an error to Sara T. Yazdi's name. The corrected version reposted with the issue on September 2, 2024.